



Paradoxical function of orexin/hypocretin circuits in a mouse model of Huntington's disease

Rhîannan H. Williams, A. Jennifer Morton, Denis Burdakov *

Department of Pharmacology, University of Cambridge, Tennis Court Road, Cambridge CB2 1PD, UK

ARTICLE INFO

Article history:

Received 18 November 2010

Revised 4 February 2011

Accepted 7 February 2011

Available online 13 February 2011

Keywords:

Hypocretin

Orexin

Hypothalamus

Sleep

Reward

Huntington's disease

Neurodegeneration

R6/2 mouse

Histamine

Glucose

ABSTRACT

Huntington's disease (HD) is a neurodegenerative disorder involving progressive motor disturbances, cognitive decline, and desynchronized sleep–wake rhythms. Recent studies revealed that restoring normal sleep–wake cycles can improve cognitive function in HD mice, suggesting that some sleep/wake systems remain operational and thus represent potential therapeutic targets for HD. Hypothalamic neurons expressing orexins/hypocretins (orexin neurons) are fundamental orchestrators of arousal in mammals, but it is unclear whether orexin circuits operate normally in HD. Here we analyzed the electrophysiology, histology, and gene expression of orexin circuits in brain slices from R6/2 mice, a transgenic model of HD with a progressive neurological phenotype. We report that in R6/2 mice, the size of an electrically distinct subpopulation of orexin neurons is reduced, as is the number of orexin-immunopositive cells in some hypothalamic regions. R6/2 orexin cells display altered glutamatergic inputs, and have an abnormal circadian profile of activity, despite normal circadian rhythmicity of the suprachiasmatic nucleus (SCN), the “master clock” of the brain. Nevertheless, even at advanced stages of HD, intrinsic firing properties of orexin cells remain normal and suppressible by serotonin, noradrenaline, and glucose. Furthermore, histaminergic neurons (key cells required for the propagation of orexin-induced arousal) also display normal responses to orexin. Together, these data suggest that the orexin system remains functional and modifiable in HD mice, although its circadian activity profile is disrupted and no longer follows that of the SCN.

© 2011 Elsevier Inc. All rights reserved.

Introduction

Huntington's disease (HD) is an inherited progressive neurodegenerative disorder caused by a CAG repeat expansion mutation in the *HTT* gene causing a polyglutamine repeat expansion in the huntingtin protein (The Huntington's Disease Collaborative Study Group, 1993). The exact function of huntingtin is unclear, although it has been implicated in many aspects of cellular function, including vesicle trafficking, axonal transport, signaling, transcriptional regulation, and mitochondrial dynamics (Cattaneo et al., 2005; Feany and La Spada, 2003; Reddy et al., 2009). The presence of the HD mutation results in abnormal movement coordination, psychiatric disturbances, weight loss, and cognitive decline (Bates et al., 2002; Kumar et al., 2010). The R6/2 transgenic mouse is one of the best characterized animal models of HD. It expresses a fragment of the HD gene and displays symptoms that recapitulate some of those seen in human HD patients (Carter et al., 1999; Lione et al., 1999; Mangiarini et al., 1996). Recently, it was found that both R6/2 mouse and human HD patients display disrupted sleep–

wake rhythms that become increasingly fragmented with disease progression (Morton et al., 2005). Because disrupted sleep is known to be deleterious to mental function, we proposed that restoration of normal sleep–wake rhythms might bring cognitive benefits to HD patients. Consistent with this idea, pharmacological or behavioral regularization of the sleep–wake cycle has been shown to improve cognitive function in R6/2 mice (Pallier et al., 2007; Pallier and Morton, 2009). However, a fundamental question relevant for informed design of such therapies remains unanswered: which components of the normal sleep–wake system are retained and which are lost in HD?

In mammals, the timing of sleep and wakefulness is profoundly affected by changes in the activity of the brain orexin/hypocretin system. Orexins/hypocretins are neurotransmitters made by a small group of hypothalamic neurons (de Lecea et al., 1998; Sakurai et al., 1998). Orexin neurons provide major inputs to arousal centers, where orexins are released and act on two specific G-protein coupled receptors (Peyron et al., 1998; Sakurai et al., 1998). Increased firing of orexin neurons stimulates wakefulness (Adamantidis et al., 2007). This is of such critical importance for consolidating normal sleep–wake rhythms that loss of orexin cells causes narcolepsy/cataplexy in dogs, mice, and humans (Hara et al., 2001; Thannickal et al., 2000).

Studies of orexin levels in the extracellular space and/or of orexin peptide content of fixed hypothalamic tissue provided conflicting information as to whether orexin circuits function normally or

* Corresponding author.

E-mail address: dib22@cam.ac.uk (D. Burdakov).

Available online on ScienceDirect (www.sciencedirect.com).

abnormally in HD (Baumann et al., 2006; Gaus et al., 2005; Meier et al., 2005; Petersen et al., 2005). If the orexin system is functional, it can potentially be manipulated to improve sleep–wake rhythms in HD. If its function is lost, orexin replacement therapies could be of benefit. Here, to distinguish between these possibilities, we examined three key aspects of orexin circuit function in HD: electrophysiological activity, peptide expression in cell bodies and axon terminals, and circadian variations in orexin cell activity.

Materials and methods

Identification of neurons

All animal procedures were performed in accordance with Animals (Scientific Procedures) Act 1986 (UK), and complied with EC Directive 86/609/EEC. Mice transgenic for eGFP in the orexin neurons (Burdakov et al., 2006) were crossed with R6/2 mice carrying exon 1 of the HD gene and a CAG repeat of 250 (Morton et al., 2009), to create R6/2 animals in which orexin neurons are specifically labeled with eGFP (R6/2-orexin-eGFP mice). Animals were genotyped by performing PCR on tail snips and CAG repeat lengths were measured by Laragen, USA. CAG repeat length of the adult mice used here for electrophysiology was 261 ± 1 (mean \pm SEM, $n = 6$). All mice were housed under a 12 h light:12 h dark lighting cycle with food and water available ad libitum (Carter et al., 1999).

We performed control experiments to ensure that the results in Figs. 4 and 5 were not an artifact of eGFP labeling. In addition to the recordings from R6/2-orexin-eGFP mice shown in Figs. 4 and 5, we performed control recordings from unlabeled orexin neurons in R6/2 mice (CAG repeat length: 253 ± 3 ; $n = 9$). In these control experiments, orexin neurons were identified by electrical fingerprints and post-recording immunocytochemistry, as in our previous studies

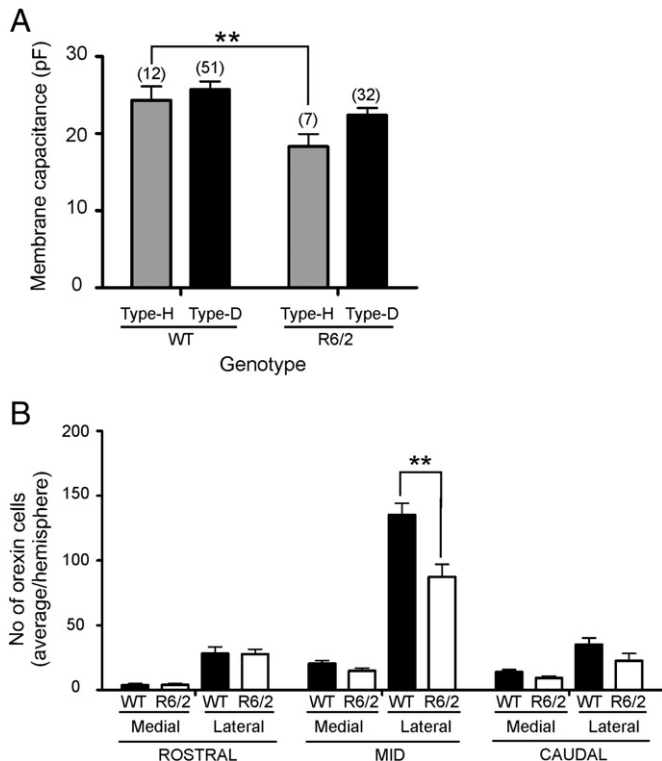


Fig. 1. Size and number of R6/2 orexin neurons. A. Size (expressed as membrane capacitance) of Type-H and Type-D orexin cells in orexin-eGFP (WT) and R6/2-orexin-eGFP (R6/2) cells (two-way ANOVA, $F(1,98) = 6.75$; $**p = 0.01$, n numbers are shown above corresponding bars). B. Number of orexin-immunoreactive cells in different regions of the tubular hypothalamus in WT and R6/2 mice (repeated measures ANOVA with Newman–Keuls multiple comparison test, $F(2,84) = 5.50$; $**p = 0.006$).

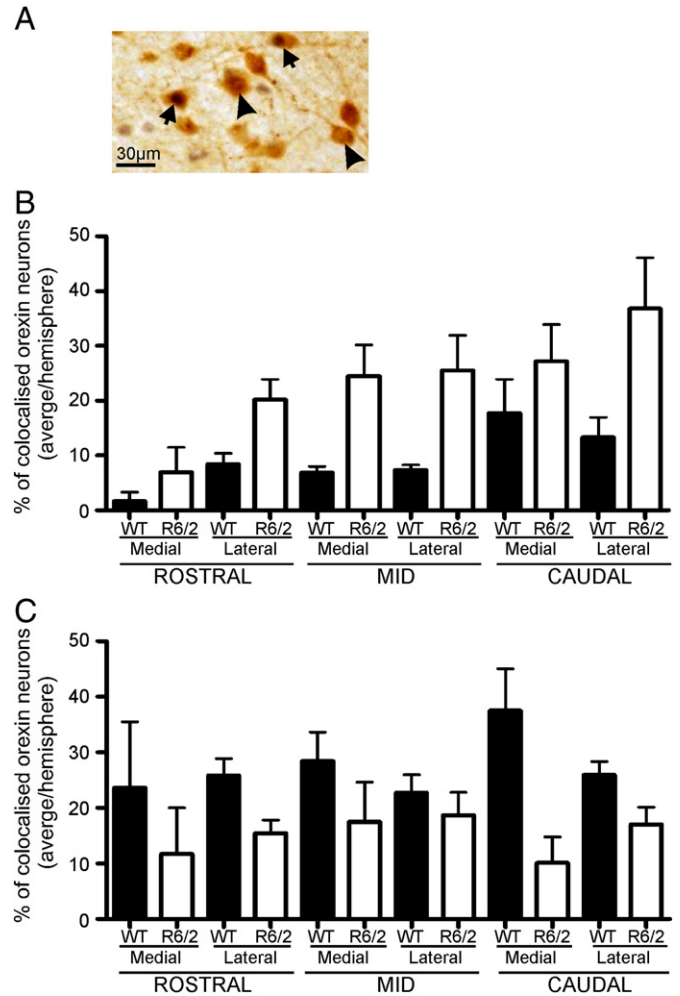


Fig. 2. Circadian activity profiles of orexin neurons in R6/2 mice. A. Example micrograph of orexin (brown) and c-Fos (black) staining used in the analysis (arrows, c-Fos positive cells; arrowheads, c-Fos negative cells). B. Percentages of orexin-immunoreactive neurons containing c-Fos immunoreactivity in different regions of the tubular hypothalamus at midday (ZT6). Repeated measures ANOVA shows that there is a significant difference between genotypes ($F(1,24) = 14.1$; $p < 0.001^{***}$) although differences specific to particular regions of the tubular hypothalamus were not detected ($F(2,24) = 0.26$; $p = 0.77$, $n = 12$ /genotype). C. Percentages of orexin-immunoreactive neurons containing c-Fos immunoreactivity in different regions of the tubular hypothalamus at midnight (ZT18). Repeated measures ANOVA revealed a significant difference between genotypes ($F(1,24) = 6.96$; $p < 0.01^{**}$) but no differences specific to particular regions of the tubular hypothalamus were detected ($F(2,24) = 0.29$; $p = 0.75$, $n = 12$ /genotype).

(Burdakov et al., 2005). The basic electrical properties and neuromodulator responses of unlabeled orexin cells in R6/2 mice were not different from those of orexin cells in R6/2-orexin-eGFP mice. R6/2 mice (CAG repeat length: 211 ± 13 ; $n = 4$) were used for the TMN experiments. All WT mice used were littermate controls.

Electrophysiology

Mice used for electrophysiology were sacrificed during the light phase. Coronal brain slices ($\sim 250 \mu\text{m}$ thick) were prepared from adult (> 14 weeks of age) mice as previously described (Williams et al., 2007), except that slicing was performed in a low-Na, low-Ca, high-sucrose solution, which contained (in mM): NaCl, 95; KCl, 1.8; KH_2PO_4 , 1.2; MgSO_4 , 7; NaHCO_3 , 26; glucose, 15; sucrose, 50; CaCl_2 , 0.5; $\text{pH} = 7.3$. Whole-cell patch-clamp recordings from eGFP-containing cells were performed as previously described (Williams et al., 2007). Recordings were done at 37°C in standard ACSF (in mM): NaCl, 125; KCl, 2.5; MgCl_2 , 2; CaCl_2 , 2; NaH_2PO_4 , 1.2; NaHCO_3 , 21; glucose, 1 (unless otherwise

stated); pH = 7.3. Bicarbonate-buffered solutions were gassed continuously with 95% O₂, and 5% CO₂. Intracellular pipette solution contained (in mM): K-gluconate, 120; KCl, 10; EGTA, 1; HEPES, 10; K₂ATP, 4; Na₂ATP, 1; MgCl₂, 2; pH = 7.3 with KOH. Data were collected using an EPC-9 HEKA amplifier and Pulse software (HEKA, Lambrecht, Germany). Electrical signals were filtered at 3 kHz and digitized at 10 kHz. Data were analyzed with Pulsefit (HEKA, Lambrecht, Germany) and Origin (Microcal, Northampton, MA) software. Action potential frequencies (Fig. 4B) and membrane potential values (Fig. 4C) were measured in current-clamp with zero holding current, 5 min after the establishment of the whole-cell configuration. Membrane potential values (Fig. 4C) were taken as the average membrane potential values during the 6th minute of whole-cell recording. Breaks in some long-duration current-clamp traces (e.g. in Figs. 5A–C, and 7B) correspond to pauses during which additional measurements (e.g. of input and access resistance) were taken.

Glutamatergic spontaneous synaptic currents (Fig. 6) were recorded at the reversal potential for GABA-A receptor-mediated current (−60 mV with our solutions), and their AMPA receptor identity verified by kinetic analysis (time to decay to 63% of peak amplitude below 6 ms) and blockade with 10 μM CNQX. 200 synaptic events/cell were analyzed. Control experiments showed that the rise times of synaptic currents were not significantly different between genotypes, suggesting that differences shown in Fig. 6 are unlikely to be due to differences in membrane capacitance. Synaptic events were analyzed using Minianalysis (Synaptosoft, Dacatur, GA, USA) and Matlab (Mathworks, Natick, MA, USA).

Two-way ANOVA with a Bonferroni post hoc test was used to compare capacitance, firing frequency, baseline membrane potential, and spike ratio measurements from orexin neurons (Prism 5,

Graphpad software Inc). A chi-squared test was used to compare the prevalence of Type D and Type H orexin neurons between WT and R6/2-orexin-eGFP mice. The effects of glucose, noradrenaline and serotonin on orexin cells were analyzed using a one-way ANOVA with Newman–Keuls multiple comparison post hoc test, and the effect of orexin-A application on histaminergic TMN neurons was compared using an unpaired *t*-test (Prism 5, Graphpad software Inc).

Chemicals

All chemicals were obtained from Sigma. Drugs were dissolved in ACSF before bath application. To prevent oxidation of noradrenaline, 10 μM of sodium metabisulphite was added (Na₂S₂O₅/NaHSO₃). Both serotonin and noradrenaline solutions were kept covered to exclude light, except when circulating in the perfusion system.

Immunohistochemistry

Tissue preparation and labeling

R6/2 mice of CAG repeat length 257.2 ± 1.2 (n = 8) and WT mice (n = 8) were killed by cervical dislocation and decapitation at either ZT6 (n = 4/genotype) or ZT18 (n = 4/genotype). The brains were removed quickly and placed into ice-cold fixative (4% paraformaldehyde/0.1 M phosphate buffered saline (PBS)) for 4 days at 4 °C. Tissue was then cryoprotected in 30% sucrose/0.1 M PBS, and cut coronally (30 μm thick slices) on a freezing sledge microtome (American Optics). Four serial sets of sections were taken per brain and stored in an antifreeze solution at −20 °C. A serial set of sections from each animal was stained for either: 1) orexin-A only (1:2000, polyclonal goat anti-orexin, Chemicon), 2) c-Fos only (1:8000 polyclonal rabbit anti-c-Fos, Santa Cruz Biotechnology), or 3) double-stained for orexin-A and c-Fos. All sections were quenched for endogenous peroxidase activity (1.5% hydrogen peroxide) before being placed in blocking solution (1% BSA/0.5% donkey serum) for 60 min. Sections were incubated overnight in the corresponding primary antibody before incubation in secondary biotinylated IgG antibody for orexin-A (1:400 donkey anti-goat; Jackson ImmunoResearch, West Grove, PA, USA) or c-Fos (1:400 donkey anti-rabbit; Jackson ImmunoResearch, West Grove, PA, USA) for 1 h. Bound antibody was visualized using the ABC system (1:400; Vector Laboratories, Peterborough, UK). For orexin-A detection, diaminobenzidine chromagen (DAB; Vector kit, Vector laboratories) was used to produce a brown reaction, and for c-Fos, nickel-intensified diaminobenzidine chromagen (NiDAB, Vector Kit; blue/black chromatic reaction). Both detection reactions were quenched in dH₂O. Sections were washed, mounted on gelatin-coated slides and air-dried. Slides were dehydrated through a series of graded ethanol baths (70%, 95% and 2 × 100%), cleared in HistoClear (National Diagnostics, Hull, UK) and cover-slipped. Slides were viewed as described in Marston et al., 2008. Areas of interest were restricted to the SCN and tuberal hypothalamus, as depicted in the stereotaxic mouse brain atlas (Paxinos and Franklin, 2001).

Quantification of orexin and c-Fos immunoreactivity

To quantify the number of orexin and/or c-Fos positive neurons, cells were counted by an investigator blind to the experimental conditions. From each animal, two sections per rostral, mid and caudal axis of the tuberal hypothalamus were analyzed (six sections total; bregma −0.82 mm to −2.06 mm, our control experiments with orexin-specific antibodies (Burdakov et al., 2005) showed that this bregma range encompasses the entire rostrocaudal extent of the orexin field in the mouse). Analyses of medial and lateral subdivisions of the tuberal hypothalamus were carried out as in our previous work (Marston et al., 2008). Total c-Fos, total orexin, and the number of colocalized orexin cells with c-Fos were counted. Immunostaining is expressed as the average value/hemisphere/group. To compare the activation profile of orexin neurons in relation to the central circadian

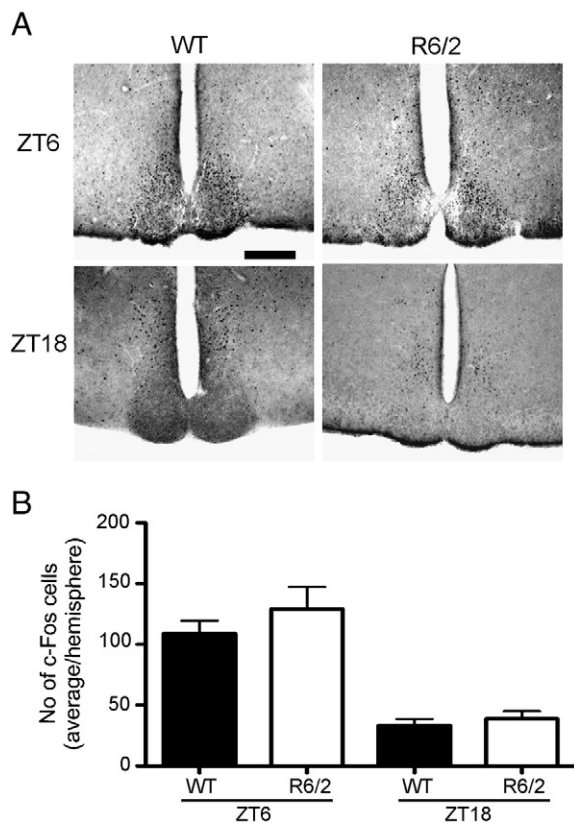


Fig. 3. Circadian activity profiles of SCN neurons in R6/2 mice. A. Examples of micrographs showing c-Fos expression (seen as dark dots) in the SCN of WT and R6 mice at ZT6 and ZT18. The scale bar is 200 μm and applies to all sections. B. Amounts of c-Fos immunoreactive cells in the SCN of WT and R6 mice at ZT6 and ZT18. There was no significant difference in c-Fos expression between genotypes (repeated measures ANOVA, $F(1,8) = 1.43$; $p = 0.27$) but a significant circadian variation was seen in both, with higher c-Fos at ZT6 (repeated measures ANOVA, $F(1,8) = 62.19$; $p < 0.0001$).

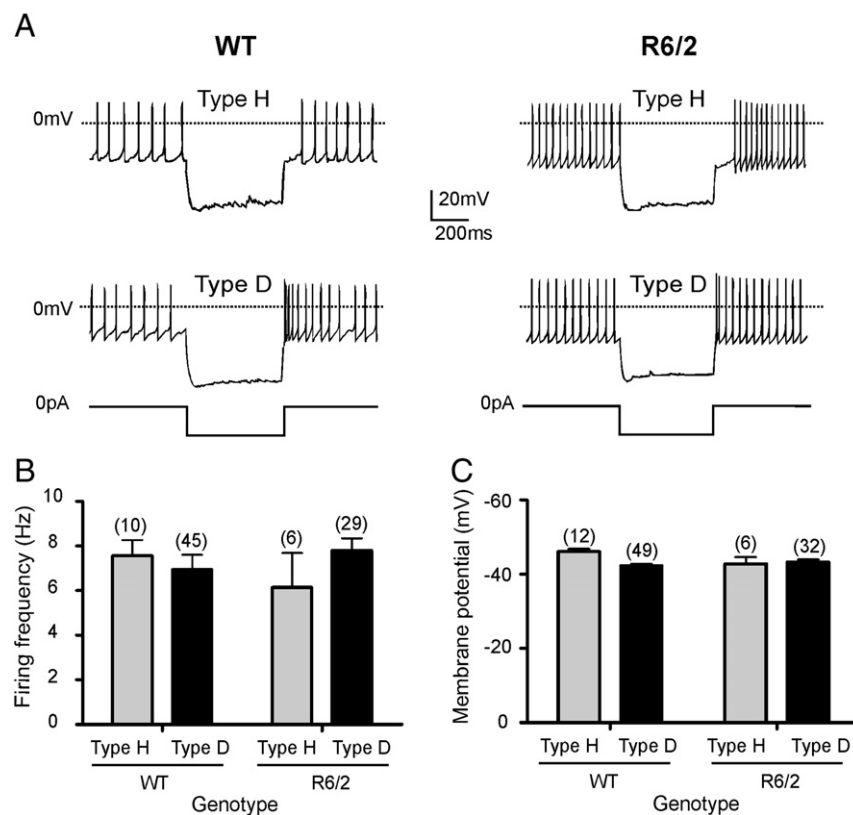


Fig. 4. Intrinsic electrical properties of R6/2 orexin neurons. A. “Type-D” (post-inhibitory excitation) and “Type-H” (post-inhibitory inhibition) orexin neurons are present in both WT (orexin-eGFP mice left) and R6/2 (R6/2-orexin-eGFP mice, right), in similar proportions (D:H = 59:14 and 36:6 cells respectively, $\chi^2 = 0.44$; $p = 0.51$). The current-clamp injection protocol is shown schematically below the traces. B. Firing frequencies in WT and R6/2 cells (mean \pm SEM); no significant differences between genotypes were observed (two-way ANOVA, $F(1,86) = 0.24$; $p = 0.78$, n numbers are shown above corresponding bars). C. Membrane potentials in WT and R6/2 cells (mean \pm SEM); no significant differences between genotypes were observed (two-way ANOVA, $F(1,95) = 1.2$; $p = 0.26$; n numbers are shown above corresponding bars).

clock, we assessed c-Fos expression in the SCN. Two rostral-medial SCN sections (bregma -0.34 mm to -0.58 mm) were analyzed per animal and the number of c-Fos positive neurons counted.

To quantify the amount of orexin-immunoreactive fibers in the TMN, we used a length-density method modified from Eckersell et al., 1998. The method was based on superimposing a grid of lines onto images of TMN, and counting the number of intersections between the orexin-immunoreactive processes and the lines (Fig. 7C). The same grid (area = 1.88 mm², total line length = 4.23 mm) was placed onto the same anatomical position in WT and R6/2 slices. Fiber density (Fig. 7D) was defined as the number of intersections per 100 mm of grid line. Four sections per animal, bregma -2.20 mm to -2.60 mm (Takahashi et al., 2006) were analyzed ($n = 6$ /genotype).

Immunohistochemical data were analyzed with a repeated-measures ANOVA and Newman-Keuls multiple comparison post hoc test (Statistica 9.0, StatSoft Inc).

Results

Size and number of orexin neurons

To compare the sizes of individual orexin neurons in HD and WT animals, we measured whole-cell membrane capacitance, which is directly proportional to membrane area (Koch, 1999). The membrane capacitance of Type-D orexin neurons (Type-D and Type-H terms refer to electrical subtypes of orexin neurons, described in Williams et al., 2008) was not significantly different between WT and HD mice (Fig. 1A, statistical analyses are provided in the figure legends). In contrast, we observed a significant reduction in the capacitance of Type-H orexin neurons in HD mice (Fig. 1A). This suggests a selective loss of membrane in Type-H orexin cells in HD. To estimate the

relative numbers of orexin-expressing neurons in WT and HD mice, we counted orexin-immunoreactive neurons in the tuberal hypothalamus. Because the lateral and medial parts of the tuberal hypothalamus have been hypothesized to contain functionally different populations of orexin neurons (Harris and Aston-Jones, 2006), we looked at different hypothalamic areas separately. Since orexin expression is correlated to the sleep-wake cycle (España et al., 2003; Estabrooke et al., 2001; Kodama et al., 2005; Marston et al., 2008; Martinez et al., 2002), we sampled two time-points (ZT6 and ZT18, 4 mice/genotype/time-point) and examined orexin immunoreactivity. We found that the number of orexin-immunoreactive neurons in the lateral portion of the tuberal hypothalamus was significantly reduced (Fig. 1B).

Day-night activity profiles of orexin and SCN neurons

In WT mice (which are nocturnal), orexin neurons have been reported to be more active during the dark phase and less active during the light phase (España et al., 2003; Estabrooke et al., 2001; Kodama et al., 2005; Marston et al., 2008; Martinez et al., 2002). To see if this was also the case in HD mice, we compared the numbers of c-Fos-immunoreactive orexin neurons from mice killed in the dark and light phases (Fig. 2). We found that during the light phase (ZT6), there was a significant difference between genotypes. The percentage of c-Fos-positive orexin neurons in R6/2 mice was higher than in WT mice (Fig. 2B, $p < 0.001$, repeated measures ANOVA with Newman-Keuls comparison post-hoc test). In contrast, during the dark phase (ZT18), there was a trend towards higher c-Fos expression in WT than in R6/2 mice, although the difference between genotypes was smaller than at ZT6 (Fig. 2C, $p < 0.01$).

To examine whether the abnormal circadian activity profile seen in orexin neurons is a general feature of sleep/wake systems in HD, we

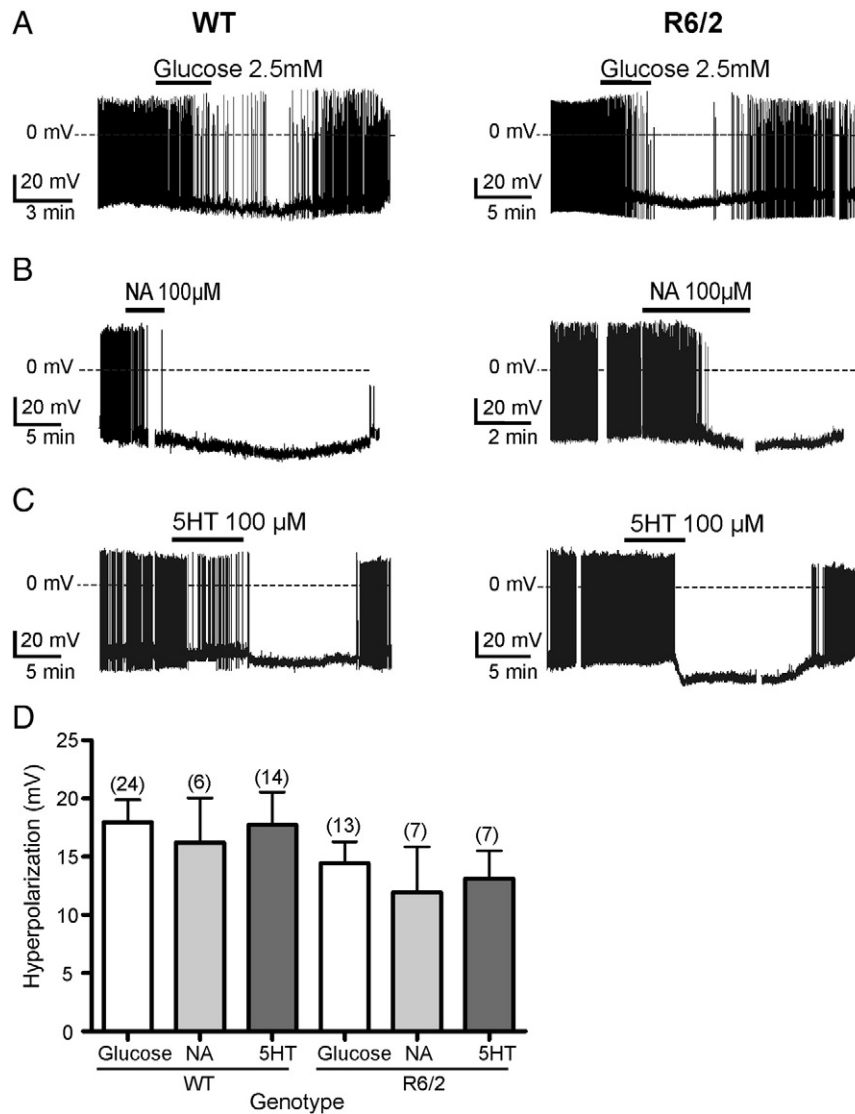


Fig. 5. Responses of R6/2 orexin neurons to inhibitory neuromodulators. Examples of responses to glucose (A), noradrenaline (B), and serotonin (C) in orexin-eGFP (WT) and R6/2-orexin-eGFP (R6/2) cells. D, statistical summary of all responses (means \pm SEM); no significant differences in hyperpolarization induced by any of the modulators was observed between genotypes (one-way ANOVA, $F(5,65) = 0.83$; $p = 0.53$, n numbers are shown above corresponding bars).

also examined the circadian variation of c-Fos expression in the suprachiasmatic nucleus, the “master timekeeper” of the brain that is thought to control activity rhythms in other brain circuits (Moore, 1995; Moore and Eichler, 1972; Stephan and Zucker, 1972). Surprisingly, given the differences we saw in orexin neurons, the levels of c-Fos expression in the SCN were normal in R6/2 mice at ZT6 and ZT18 (Fig. 3), suggesting that the abnormal activation levels in the orexin system are not a result of an abnormal SCN clock.

Intrinsic electrical activity of orexin neurons

We compared the intrinsic electrical properties of living orexin neurons (identified by targeted eGFP expression, see [Materials and methods](#)) from age and litter-matched wild-type (WT) mice and R6/2 mice in advanced stages of their disease (>14 week old mice). The healthy orexin system is electrophysiologically dichotomous, and is made up of Type D or Type H orexin cells that differ in their membrane properties (Williams et al., 2008). We found that the same electrical dichotomy persisted in the HD orexin system (Fig. 4A). Specifically, the relative proportions of “D” and “H” orexin cells were D: H = 86:14% of 42 cells tested from 6 R6/2 mice and 81:19% of 73 cells tested from 9 WT mice. The intrinsic firing rates of orexin

neurons from R6/2 brains were not significantly different from those in WT brains (Fig. 4B). Healthy orexin neurons are also characterized by relatively depolarized membrane potentials (Eggermann et al., 2003; Yamanaka et al., 2003b), and this feature was not significantly different in WT and R6/2 orexin neurons (Fig. 4C).

Effects of neurotransmitters and neuromodulators on orexin neurons

The electrical activity of healthy orexin neurons is controlled by a number of physiological modulators, such as glucose, monoamines, and glutamate (Burdakov et al., 2005; Yamanaka et al., 2003a, 2003b). Since the spontaneous electrical activity of orexin cells from R6/2 mice appeared normal (Fig. 4), it may be that the responsiveness of orexin cells to these modulators becomes altered in HD and contributes to abnormal circadian activity of orexin cells and to poor sleep/wake cycles. However, we found that both WT and R6/2 orexin neurons exhibited specialized inhibitory responses to small elevations in extracellular glucose comparable to those that occur in the brain after eating (e.g. change from 1 mM to 2.5 mM, Fig. 5A). Apart from glucose, the activity of WT orexin neurons can also be directly modulated by noradrenaline and serotonin (Yamanaka et al., 2003b). We found that R6/2 orexin neurons were able to exhibit robust

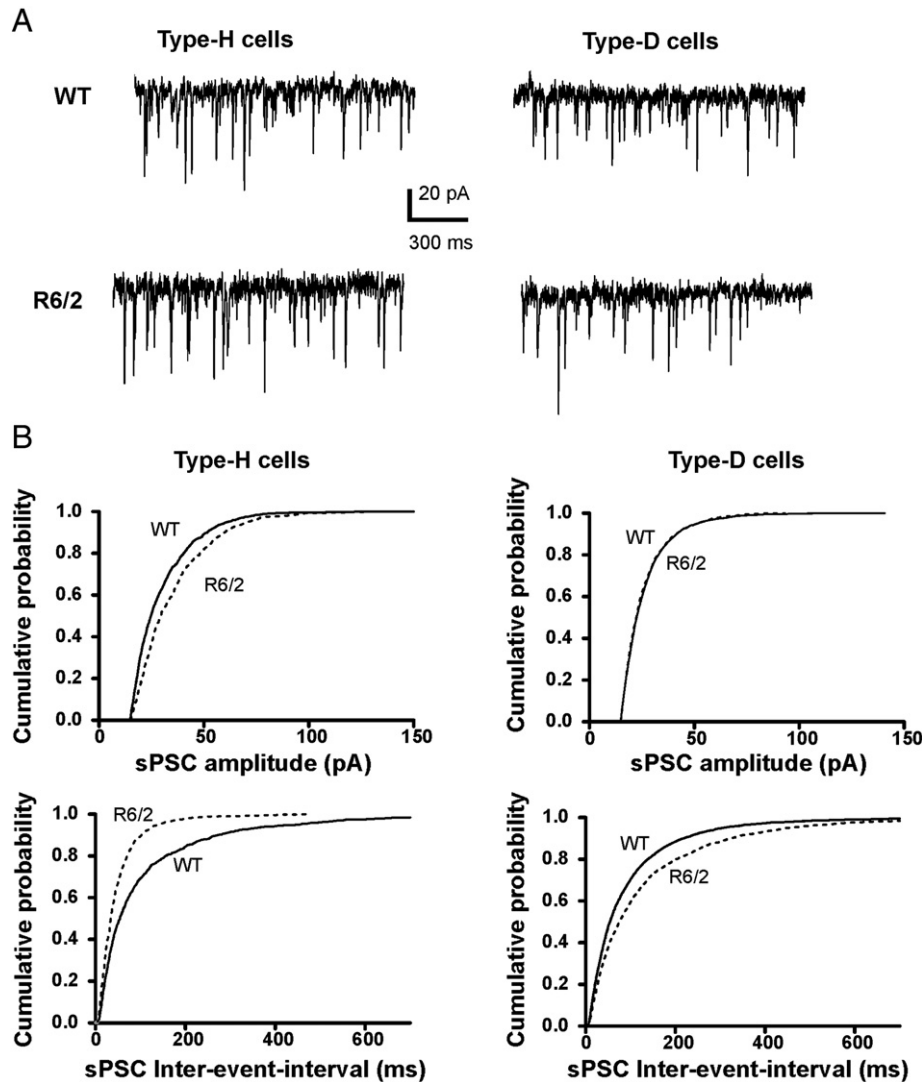


Fig. 6. Excitatory synaptic currents in R6/2 orexin neurons. Spontaneous glutamatergic postsynaptic currents (sPSC) recorded from orexin neurons in WT and R6/2 mice. A. Typical voltage-clamp traces showing sPSCs recorded at -60 mV (see Methods). B. Cumulative probability plots of sPSC amplitudes (top) and frequencies (bottom). Top left, in R6/2 mice Type-H cells sPSCs had significantly larger amplitudes compared to WT cells ($n = 4$ and 7 cells respectively, $p < 0.001$ by K-S test). Top right, in Type-D cells, sPSC amplitudes were not significantly different between R6/2 and WT cells ($n = 13$ and 21 cells respectively, $p > 0.2$ by K-S test). Bottom left, in R6/2 mice Type-H cells sPSCs had significantly smaller inter-event-intervals (i.e. higher frequencies) compared to WT cells ($n = 4$ and 7 cells respectively, $p < 0.001$ by K-S test). Bottom right, in R6/2 mice Type-D cells sPSCs had significantly larger inter-event-intervals (i.e. lower frequencies) compared to WT cells ($n = 4$ and 7 cells respectively, $p < 0.001$ by K-S test).

responses to these transmitters (Figs. 5B and C). The amplitudes of the hyperpolarizing membrane responses to glucose, noradrenaline, and serotonin were not significantly different in WT and R6/2 mice (Fig. 5D). In contrast, we found that both the frequency and the amplitude of spontaneous glutamatergic synaptic currents were significantly increased in Type H orexin cells in R6/2 mice (Fig. 6). Thus, while a subset of R6/2 orexin neurons receives abnormally high excitatory synaptic drive, their activity can still be effectively constrained by inhibitory modulators (see Discussion).

Responses of wakefulness-regulating neurons to orexin

Histamine-containing neurons of the tuberomammillary hypothalamus are thought to be a major pathway through which the activity of orexin neurons promotes cognitive arousal (Eriksson et al., 2001). In healthy brains, histamine neurons are excited by orexin through activation of the orexin type-2 receptor (Eriksson et al., 2001). To examine whether this interaction between the orexin and histamine system is present in HD brains, we identified living histamine neurons in R6/2 mice (Fig. 7A), and analyzed their

responses to bath-applied orexin-A. As in previous studies, histaminergic neurons were identified by their well-characterized distinctive properties (Fig. 7A), such as: i) large diameter (20 – 30 μ m) and multipolar shape; ii) a large I_H -mediated sag upon membrane hyperpolarization; iii) prominent spike after-hyperpolarization; iv) tonic spontaneously firing (Haas et al., 1989; Haas and Reiner, 1988; Stevens et al., 2001). Application of orexin-A elicited robust and reversible depolarization and stimulation of firing in histamine neurons in both WT and R6/2 mice (Fig. 7B, no significant difference between phenotypes, statistics are given in the figure legend). This suggests that the orexin receptor signaling is preserved in brains affected by the HD mutation. Orexin-containing fibers also remained present in the tuberomammillary nucleus of R6/2 mice, although their density was reduced compared with WT mice (Figs. 7C and D).

Discussion

We found that, despite the marked abnormalities of rest-activity cycles in R6/2 mice, the orexin neurons in R6/2 mouse brain function normally in vitro. Their resting firing rates and intrinsic biophysical

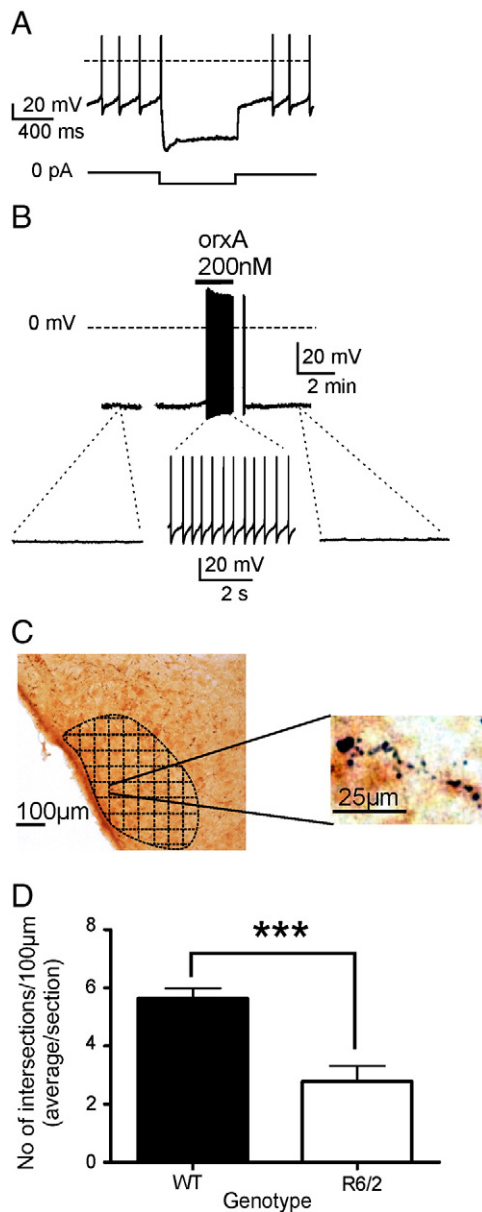


Fig. 7. Interactions between the orexin and histamine systems in R6/2 mice. **A.** Example of the electrical fingerprint used to identify histaminergic neurons (see text for details). The current-clamp protocol is shown schematically below the trace. **B.** Example of orexin-A-induced depolarization and excitation in an R6/2 histamine neuron (all cells were held at -50 mV to standardize quantification of responses). Orexin-induced depolarization was (mean \pm SEM): 4.57 ± 0.54 mV ($n = 12$) in WT mice and 5.2 ± 0.81 mV ($n = 11$) in R6/2 mice; no significant differences were detected (unpaired t -test, $t(21) = 0.6$; $p = 0.52$). **C.** Example of raw data used to quantify orexin fiber density in the TMN. Left, low-magnification picture of the TMN with the analysis grid superimposed (see Methods). Right, an orexin-immunoreactive fiber shown at high magnification. **D.** Orexin fiber densities in the TMN of WT and R6/2 mice. There was a significant reduction in fiber density in the TMN of R6/2 mice (repeated-measures ANOVA, $F(1, 10) = 7.16$; $p = 0.023^*$, $n = 6/\text{genotype}$).

properties are normal and they respond characteristically to inhibitory neuromodulators such as serotonin, noradrenaline and glucose. Furthermore, the orexin responsiveness of one of the projection targets of orexin neurons is also normal. Similar to that found by Petersen et al. 2005, we found a reduction in orexin cell size and number, although there were differences in the magnitude of orexin cell loss ($\sim 30\%$ in ours vs $\sim 70\%$ in Petersen et al., 2005) that we attribute to the use of R6/2 mice with different numbers of CAG repeats (Morton et al., 2009). However, neither the orexin cell loss in R6/2 mice in our study, nor that seen in human HD patients ($\sim 30\%$;

Petersen et al., 2005), is likely to be sufficient to produce the severe disintegration of the rest-activity cycles. This is because a much greater orexin cell loss is likely to be needed to produce severe sleep/wake abnormalities and metabolic dysfunction (Gerashchenko et al., 2003; Hara et al., 2001). Rather, our data contribute to a growing body of evidence suggesting that disordered brain circuitry causes abnormal behavior before there are major abnormalities in neuronal function in any one particular group of cells (Cepada et al., 2006; Maywood et al., 2010; Paulsen, 2009).

The regulation of rest-activity cycles in mammals is complex, and orchestrated by a number of overlapping and interacting pathways. Orexins are key stimulators of arousal, although their precise role in sleep and wakefulness remains to be established. Orexin production and neuronal activity is regulated in a circadian manner (Fenzl et al., 2009; Marston et al., 2008), and is in turn required for some circadian behaviors, such as the circadian control of rapid eye movement sleep (Kantor et al., 2009). Interestingly, we found that the circadian activity pattern of c-Fos activation in orexin neurons in R6/2 mice was abnormal. This contrasts with data from SCN neurons, which displayed a similar activity pattern in R6/2 and WT mice. Because we only looked at two time points, it was not possible to tell whether the circadian variation of orexin cell activity was blunted or phase-shifted. However, either of these possibilities would be consistent with abnormal circadian regulation of gene expression already described in R6/2 mice. We have previously described both blunted expression of some genes (e.g. clock output genes in the brain and liver; Maywood et al., 2010; Morton et al., 2005) and phase shifts in expression of mPer2 between the SCN and other parts of the brain (Maywood et al., 2010). Interestingly, the loss of normal circadian variation in orexin cell activity that we observed may explain the apparently conflicting data in the field, where some studies have found abnormalities in orexin levels (Petersen et al., 2005), whereas others have found orexin levels to be normal (Baumann et al., 2006; Gaus et al., 2005; Meier et al., 2005). If the circadian regulation of orexin cell activity is abnormal (rather than the overall levels of activity), then the time-of-day of sampling, which is rarely controlled as a variable in human sampling, becomes critically important, since abnormalities may be obvious in some individuals at particular times of the circadian cycle but not apparent at other times.

The loss of circadian control revealed by our results suggests there is a gain-of-function in orexin during the normal rest period (the light phase for mice) when orexin cell activity is normally at its nadir, which is consistent with the cognitively detrimental hyperactivity in the R6/2 mice and human HD patients during this period. Elevated activity of R6/2 orexin cells during the light phase could, in theory, result from either a reduced action of inhibitory modulators, and/or increased action of excitatory modulators. We found that noradrenaline had a similar (inhibitory) action on orexin cells from WT and R6/2 mice killed during the light phase. This suggests that a switch between noradrenaline-mediated excitation and inhibition (Grivel et al., 2005) is unlikely to account for the loss of circadian activity of orexin cells. On the other hand, we found that in an electrically distinct subset (Type-H) of R6/2 orexin cells from mice killed during the light phase, the amplitude and frequency of excitatory synaptic currents is abnormally high (Fig. 6B). This is consistent with overactivity of orexin cells during the light phase seen in our c-Fos experiments. However, a causal relationship between glutamatergic gain-of-function and behavioral hyperactivity requires further investigation, since we found a reduced frequency of glutamate currents in Type-D orexin cells (Fig. 6B). Interestingly, synaptic gain-of-function was also recently reported in the peripheral nervous system of another mouse model of HD (Rozas et al., 2011).

We do not know if there is a direct relationship between the changes in the orexin pathways and the disintegration of the rest-activity behavior in R6/2 mice and human HD sufferers. Nevertheless, our findings (that both orexin neurons and target neurons in the

orexin circuitry are functional) suggest that the orexin system could be an attractive therapeutic target for treating sleep/wake deficits in HD. Our results also suggest that designing treatment strategies should include careful consideration of circadian pattern of orexin cell activity, rather than focusing on a simple loss- or gain-of-function. For example, if overactivity of the orexin system during subjective night disrupts sleep, then an appropriate therapy might be to down-regulate the orexin system selectively during subjective night, rather than to administer a wakefulness stimulant during the subjective day.

Although we found that improving circadian behavior in R6/2 mice improved cognitive function, as yet, no similar studies have been conducted in HD patients. One study examined the effects of modafinil on cognitive function (Blackwell et al., 2008), but only a single dose was used, and the drug was tested during the day as a cognitive enhancer, rather than at the beginning of the wake period as a circadian modulator. Interestingly, HD patients do not necessarily self-report sleep difficulties (Goodman et al., 2010), although significant abnormalities in sleep architecture can be detected early in the time-course of their disease (Goodman et al., 2011). A better understanding of sleep and circadian abnormalities in HD patients is overdue, but it remains to be seen if there is a relationship between cognitive decline and circadian dysfunction.

Acknowledgments

AJM was the recipient of a Royal Society Leverhulme Senior Research Fellowship. This work was funded by grants to from CHDI Inc.(AJM) and the European Research Council (DB).

References

- Adamantidis, A.R., et al., 2007. Neural substrates of awakening probed with optogenetic control of hypocretin neurons. *Nature* 450, 420–424.
- Bates, G., et al., 2002. *Huntington's Disease*. Oxford University Press, Oxford.
- Baumann, C.R., et al., 2006. Hypocretin-1 (orexin A) levels are normal in Huntington's disease. *J. Neurol.* 253, 1232–1233.
- Blackwell, A.D., et al., 2008. The effects of modafinil on mood and cognition in Huntington's disease. *Psychopharmacology (Berl)* 199, 29–36.
- Burdakov, D., et al., 2005. Physiological changes in glucose differentially modulate the excitability of hypothalamic melanin-concentrating hormone and orexin neurons in situ. *J. Neurosci.* 25, 2429–2433.
- Burdakov, D., et al., 2006. Tandem-pore K⁺ channels mediate inhibition of orexin neurons by glucose. *Neuron* 50, 711–722.
- Carter, R.J., et al., 1999. Characterization of progressive motor deficits in mice transgenic for the human Huntington's disease mutation. *J. Neurosci.* 19, 3248–3257.
- Cattaneo, E., et al., 2005. Normal huntingtin function: an alternative approach to Huntington's disease. *Nat. Rev. Neurosci.* 6, 919–930.
- Cepada, C., et al., 2006. The corticospinal pathway in Huntington's disease. *Prog. Neurobiol.* 81, 253–271.
- de Lecea, L., et al., 1998. The hypocretins: hypothalamus-specific peptides with neuroexcitatory activity. *Proc. Natl Acad. Sci. USA* 95, 322–327.
- Eckersell, C.B., et al., 1998. Estrogen-induced alteration of mu-opioid receptor immunoreactivity in the medial preoptic nucleus and medial amygdala. *J. Neurosci.* 18, 3967–3976.
- Eggermann, E., et al., 2003. The wake-promoting hypocretin-orexin neurons are in an intrinsic state of membrane depolarization. *J. Neurosci.* 23, 1557–1562.
- Eriksson, K.S., et al., 2001. Orexin/hypocretin excites the histaminergic neurons of the tuberomammillary nucleus. *J. Neurosci.* 21, 9273–9279.
- Espana, R.A., et al., 2003. Fos immunoreactivity in hypocretin-synthesizing and hypocretin-1 receptor-expressing neurons: effects of diurnal and nocturnal spontaneous waking, stress and hypocretin-1 administration. *Neuroscience* 121, 201–217.
- Estabrooke, I.V., et al., 2001. Fos expression in orexin neurons varies with behavioral state. *J. Neurosci.* 21, 1656–1662.
- Feany, M.B., La Spada, A.R., 2003. Polyglutamines stop traffic: axonal transport as a common target in neurodegenerative diseases. *Neuron* 40, 1–2.
- Fenzl, T., et al., 2009. Circadian rhythms of basal orexin levels in the hypothalamus are not influenced by an impaired corticotropin-releasing hormone receptor type 1 system. *Behav. Brain Res.* 203, 143–145.
- Gaus, S.E., et al., 2005. CSF hypocretin levels are normal in Huntington's disease patients. *Sleep* 28, 1607–1608.
- Gerashchenko, D., et al., 2003. Effects of lateral hypothalamic lesion with the neurotoxin hypocretin-2-saporin on sleep in Long-Evans rats. *Neuroscience* 116, 223–235.
- Goodman, A.O., et al., 2010. Identifying sleep disturbances in Huntington's disease using a simple disease-focused questionnaire. *PLoS Curr.* 2, RRN1189.
- Goodman, A.O., et al., 2011. Asymptomatic Sleep Abnormalities Are a Common Early Feature in Patients with Huntington's Disease. *Curr. Neurol. Neurosci. Rep.* 11, 211–217.
- Grivel, J., et al., 2005. The wake-promoting hypocretin/orexin neurons change their response to noradrenaline after sleep deprivation. *J. Neurosci.* 25, 4127–4130.
- Haas, H.L., Reiner, P.B., 1988. Membrane properties of histaminergic tuberomammillary neurones of the rat hypothalamus in vitro. *J. Physiol.* 399.
- Haas, H.L., et al., 1989. The brain histamine system in vitro. *J. Neurosci. Methods* 28, 71–75.
- Hara, J., et al., 2001. Genetic ablation of orexin neurons in mice results in narcolepsy, hypophagia, and obesity. *Neuron* 30, 345–354.
- Harris, G.C., Aston-Jones, G., 2006. Arousal and reward: a dichotomy in orexin function. *Trends Neurosci.* 29, 571–577.
- Kantor, S., et al., 2009. Orexin neurons are necessary for the circadian control of REM sleep. *Sleep* 32, 1127–1134.
- Koch, C., 1999. *Biophysics of Computation*. Oxford University Press, New York.
- Kodama, T., et al., 2005. High Fos expression during the active phase in orexin neurons of a diurnal rodent, *Tamias sibiricus barberi*. *Peptides* 26, 631–638.
- Kumar, P., et al., 2010. Huntington's disease: pathogenesis to animal models. *Pharmacol. Rep.* 62, 1–14.
- Lione, L.A., et al., 1999. Selective discrimination learning impairments in mice expressing the human Huntington's disease mutation. *J. Neurosci.* 19, 10428–10437.
- Mangiarini, L., et al., 1996. Exon 1 of the HD gene with an expanded CAG repeat is sufficient to cause a progressive neurological phenotype in transgenic mice. *Cell* 87, 493–506.
- Marston, O.J., et al., 2008. Circadian and dark-pulse activation of orexin/hypocretin neurons. *Mol. Brain* 1, 19.
- Martinez, G.S., et al., 2002. Diurnal and nocturnal rodents show rhythms in orexinergic neurons. *Brain Res.* 955, 1–7.
- Maywood, E.S., et al., 2010. Disruption of peripheral circadian timekeeping in a mouse model of Huntington's disease and its restoration by temporally scheduled feeding. *J. Neurosci.* 30, 10199–10204.
- Meier, A., et al., 2005. Normal hypocretin-1 (orexin-A) levels in the cerebrospinal fluid of patients with Huntington's disease. *Brain Res.* 1063, 201–203.
- Moore, R.Y., 1995. Organization of the mammalian circadian system. *Ciba Found. Symp.* 183, 88–99 discussion 100–6.
- Moore, R.Y., Eichler, V.B., 1972. Loss of a circadian adrenal corticosterone rhythm following suprachiasmatic lesions in the rat. *Brain Res.* 42, 201–206.
- Morton, A.J., et al., 2005. Disintegration of the sleep–wake cycle and circadian timing in Huntington's disease. *J. Neurosci.* 25, 157–163.
- Morton, A.J., et al., 2009. Paradoxical delay in the onset of disease caused by super-long CAG repeat expansions in R6/2 mice. *Neurobiol. Dis.* 33, 331–341.
- Pallier, P.N., Morton, A.J., 2009. Management of sleep/wake cycles improves cognitive function in a transgenic mouse model of Huntington's disease. *Brain Res.* 1279, 90–98.
- Pallier, P.N., et al., 2007. Pharmacological imposition of sleep slows cognitive decline and reverses dysregulation of circadian gene expression in a transgenic mouse model of Huntington's disease. *J. Neurosci.* 27, 7869–7878.
- Paulsen, J.S., 2009. Functional imaging in Huntington's disease. *Exp. Neurol.* 216, 272–277.
- Paxinos, G., Franklin, K.B.J., 2001. *The Mouse Brain in Stereotaxic Coordinates*. Academic Press, San Diego.
- Petersen, A., et al., 2005. Orexin loss in Huntington's disease. *Hum. Mol. Genet.* 14, 39–47.
- Peyron, C., et al., 1998. Neurons containing hypocretin (orexin) project to multiple neuronal systems. *J. Neurosci.* 18, 9996–10015.
- Reddy, P.H., et al., 2009. Mitochondrial structural and functional dynamics in Huntington's disease. *Brain Res. Rev.* 61, 33–48.
- Rozas, J.L., et al., 2011. Increased neurotransmitter release at the neuromuscular junction in a mouse model of polyglutamine disease. *J. Neurosci.* 31, 1106–1113.
- Sakurai, T., et al., 1998. Orexins and orexin receptors: a family of hypothalamic neuropeptides and G protein-coupled receptors that regulate feeding behavior. *Cell* 92, 573–585.
- Stephan, F.K., Zucker, I., 1972. Circadian rhythms in drinking behavior and locomotor activity of rats are eliminated by hypothalamic lesions. *Proc. Natl Acad. Sci. USA* 69, 1583–1586.
- Stevens, D.R., et al., 2001. The mechanism of spontaneous firing in histamine neurons. *Behav. Brain Res.* 124, 105–112.
- Takahashi, K., et al., 2006. Neuronal activity of histaminergic tuberomammillary neurons during wake–sleep states in the mouse. *J. Neurosci.* 26, 10292–10298.
- Thannickal, T.C., et al., 2000. Reduced number of hypocretin neurons in human narcolepsy. *Neuron* 27, 469–474.
- The Huntington's Disease Collaborative Research Group, 1993. A novel gene containing a trinucleotide repeat that is expanded and unstable on Huntington's disease chromosomes. *Cell* 72 (6), 971–983.
- Williams, R.H., et al., 2007. Control of hypothalamic orexin neurons by acid and CO₂. *Proc. Natl Acad. Sci. USA* 104, 10685–10690.
- Williams, R.H., et al., 2008. Adaptive sugar sensors in hypothalamic feeding circuits. *Proc. Natl Acad. Sci. USA* 105, 11975–11980.
- Yamanaka, A., et al., 2003a. Hypothalamic orexin neurons regulate arousal according to energy balance in mice. *Neuron* 38, 701–713.
- Yamanaka, A., et al., 2003b. Regulation of orexin neurons by the monoaminergic and cholinergic systems. *Biochem. Biophys. Res. Commun.* 303, 120–129.